

# Ceramic composites with improved thermo-mechanical properties

B. A. SAVA, C. ȚÂRDEI<sup>b</sup>, I. STAMATIN<sup>c</sup>, C. NĂSTASE<sup>c</sup>, F. NĂSTASE<sup>c</sup>

<sup>a</sup>The National Institute for Glass, 47th Th. Pallady Av., s3, Bucharest, Romania

<sup>b</sup>The Research and Development Institute ICPE-CA, Bucharest, Romania

<sup>c</sup>The University of Bucharest, Physics Faculty, Măgurele, Romania

The ceramic composites from the quaternary Al<sub>2</sub>O<sub>3</sub>-SiO<sub>2</sub>-MgO-ZrO<sub>2</sub> system, with the major compounds: mullite, cordierite, zirconium silicate and silica have important applications for the dental technics, because of their interesting thermo-mechanical properties. There can be obtained materials of high purity, good homogeneity, fine precision and also very good thermo-mechanical properties (the thermal expansion coefficient  $\alpha$  from 20 to 920 °C between  $2.5$  and  $4 \times 10^{-6} \text{ K}^{-1}$ ), extremely good chemical stability, without risk related to toxic inclusions in dental materials. Several thermal treatment programs are proposed for the obtaining of the samples from ceramic composite materials of four different compositions and there is determined the influences of thermal history on the properties of the studied samples. The chemical composition influence on the thermo-mechanical properties is also studied, especially for the systems with different proportions of cordierite. The samples are investigated through the determinations of the physical and chemical properties comprising: density, porosity, water absorption, mechanical strength, thermal expansion coefficient, thermal shock resistance, chemical resistance, X-ray diffraction, Raman and FTIR Spectroscopy, Scanning Electronic Microscopy-SEM.

(Received September 4, 2006; accepted June 27, 2007)

**Keywords:** Ceramic composites, Mullite, Cordierite, Zirconium silicate, Raman, SEM, XRD, FTIR

## 1. Introduction

For dental uses, the ceramic composites must be an ideal compromise between an excellent thermal shock resistance and good physico-chemical and mechanical characteristics.

The composites based on silica contain the SiO<sub>2</sub> glass as major phase, proving excellent properties of thermal shock resistance and also contain amounts of other oxides, such as Al<sub>2</sub>O<sub>3</sub>, which improve the thermo-mechanical and chemical properties at high temperatures. The ceramic composites mullite-cordierite are made from a major mullite phase (the ceramic matrix) and variable amount of cordierite. The mullite phase improves the mechanical characteristics and increases the maximum utilisation temperature for the products. The products obtained from those composites will combine harmoniously the excellent

thermal shock resistance, given by the cordierite phase (compound with very low thermal expansion coefficient  $\alpha$ ), and the superior mechanical characteristics of the mullite phase (compound with high value for the elastic modulus). The composites based on zirconium silicate together with alumina or kaolin proves also very good thermo mechanical properties.

## 2. Experimental

The experiments were made for four composite types, two based on silica and mullite, code S and MS, the third based on mullite and cordierite, code MC and the fourth on zirconium silicate with alumina and kaolin additives, code ZSC and ZSA. The chosen compositions are presented in Table 1.

Table 1. The compositions, in gravimetric %.

Sample code	Composition [wt. %]						
	SiO <sub>2</sub>	Al <sub>2</sub> O <sub>3</sub>	CaO	Na <sub>2</sub> O	P <sub>2</sub> O <sub>5</sub>	MgO	ZrO <sub>2</sub>
S	88-90	5-6	4-5	0.5-1	0-1		
MS	53-57	35-37	1-2	2-3		3-4	
MC	35-40	53-60				4-7	
ZSC	33-35	4-5					60-63
ZSA	15-17	49-51					33-35

For slurry moulding there were added additives, sodium silicate, 3-7 % and sodium polyphosphate 0.2-0.5 %, over 100%. The raw materials were dried in electric stove, China and weighted on a 2 kg technical balance, Sibiu,  $\pm 1$  % precision. The homogenisation was realised

on humid route, in a stainless homogenizer, provided with one helicoidal stirrer.

The gypsum moulding was manually made. Four hours after the moulding, the products were manually taken out. The samples were dried in the electric stove, at  $120 \text{ °C} \pm 5 \text{ °C}$ , for 24 hours. After the drying, the samples

were burned in an electrical chamber four, Nabertherm, provided with molybdenum disilicon elements, at temperatures between 1350 and 1450 °C.

The mullite-cordierite samples were prepared in two steps: the first one comprises the cordierite fired preparation, from who, in the next step, it was realised the ceramic composite material. The homogenization of fired cordierite with the mullite was made by humid way, in plastic mills, in a planetary mill, for 6 hours. The ceramic material was prepared for semi humid pressing (humidity of 8-10 %). The used binder was an aqueous solution of polyvinyl alcohol of 5 % concentration. From this material they were realised the samples, with the aid of a hydraulic press, at 5 tone/camp. The samples were dried in the stove, at  $110^{\circ}\text{C} \pm 5^{\circ}\text{C}$ , for 12 hours. After the drying, the samples were burned in the electrical chamber four, at 1350-1430°C.

The preparation of ceramic composite materials based on zirconium silicate was similar with the technics utilised for the samples made from mullite-cordierite. They were prepared two types of materials based on zirconium silicate: ZSA base on zirconium silicate and alumina; ZSC base on zirconium silicate and kaolin. The final burning temperatures for these ceramic materials were between 1350 and 1430 °C.

For the sintered samples they were measured the density, porosity and contraction measurements, for the determination of burning parameters, through the usual methods.

The thermal expansion measurements were made with the aid of a LINSEIS L75 apparatus.

They were also made measurements of Raman spectroscopy, Raman System 2001 Ocean Optics apparatus, XRD, Dron 3, FTIR, Shimadzu and scanning electronic microscopy SEM, Philips Quanta 5 apparatus.

### 3. Results and discussion

The material and textural characteristics (density, porosity and absorbtion), are given in Table 2.

Table 2. The characteristics, at different burning temperatures.

The composite sample; sintering temperature [°C]	Apparent density, $\rho_a$ [g/cm <sup>3</sup> ]	Apparent porosity, $P_a$ [%]	Absorbti on [%]
S; 1450	1.51	33.18	17.97
S; 1400	1.50	33.63	18.22
MS; 1450	2.08	20.22	8.82
MS; 1400	2.06	20.63	9.04
MS; 1350	2.04	21.64	9.55
MC; 1430	2.56	9.50	
MC; 1400	2.08	28.35	
MC; 1375	2.03	30.17	
ZSC; 1430 °C	3.245	23.90	
ZSC; 1400 °C	3.165	25.55	
ZSC; 1350 °C	3.14	26.60	
ZSA; 1430 °C	3.255	16.75	
ZSA; 1400 °C	3.225	16.875	
ZSA; 1350 °C	3.21	19.95	

The thermal linear expansion index for the composite ceramic samples realised are presented in Table 3.

Table 3. The thermal linear expansion index, for several sintering temperatures, for the composite obtained samples.

The composite sample	The sintering temperature	The thermal linear expansion index $\alpha_{20-920^{\circ}\text{C}} \times 10^6$ [grd <sup>-1</sup> ]
S	1400 °C	1.9
MS	1400 °C	3.8
MC	1430 °C	3.3
	1400 °C	3.4
	1375 °C	3.6
ZSC	1430 °C	4.4
	1400 °C	4.5
	1350 °C	4.6
ZSA	1430 °C	5.0
	1400 °C	5.1
	1350 °C	5.3

The Raman spectra, for composite ceramic samples are presented in Fig. 1- Fig. 9.

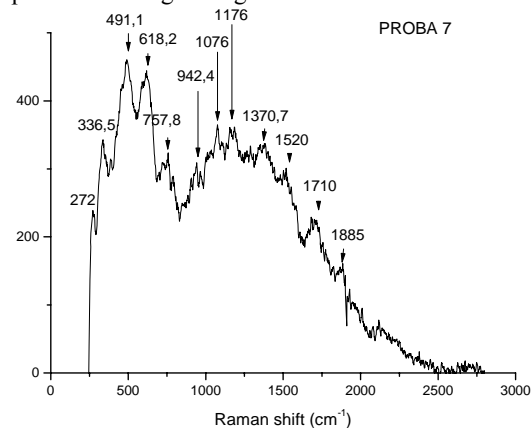


Fig. 1. The Raman spectra for the S sample.

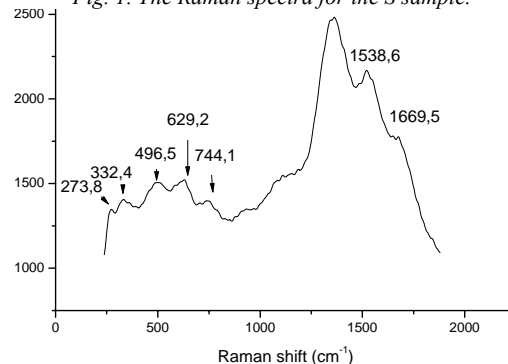


Fig. 2. The Raman spectra for the MS sample.

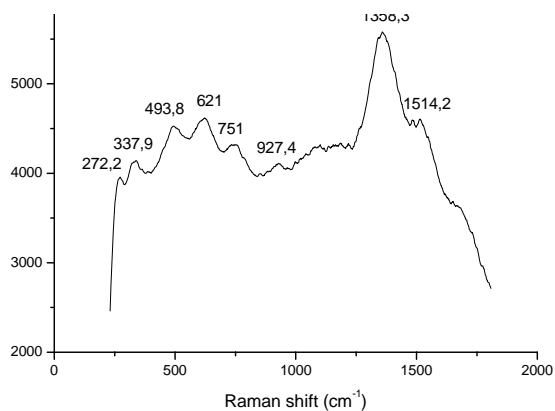


Fig. 3. The Raman spectra for the MC type sample, sintered at 1430 °C.

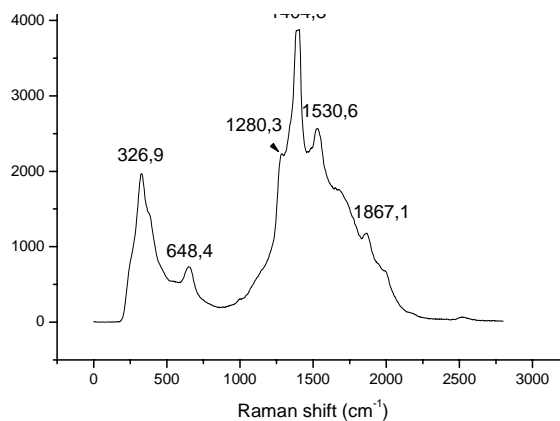


Fig. 6. The Raman spectra, for the ZSC type sample, sintered at 1400 °C.

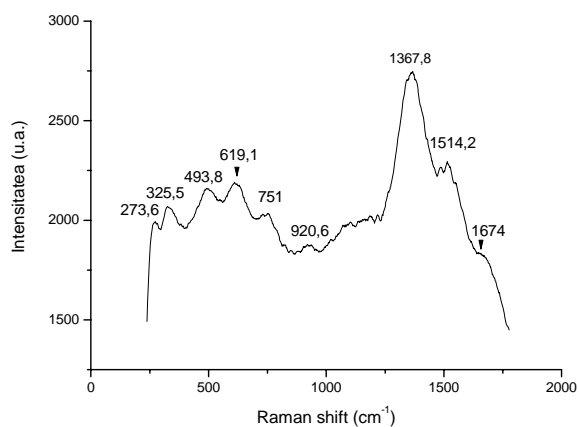


Fig. 4. The Raman spectra for the MC type sample, sintered at 1400 °C.

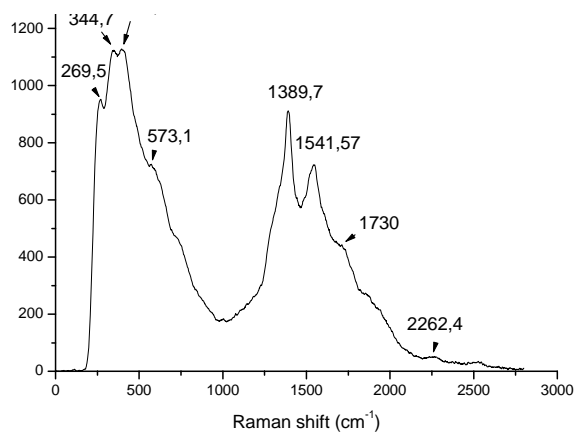


Fig. 7. The Raman spectra for the ZSA type sample, sintered at 1430 °C.

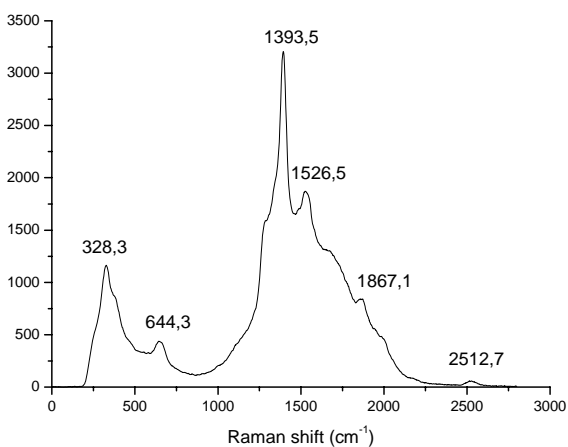


Fig. 5. The Raman spectra for the ZSC type sample, sintered at 1430 °C.

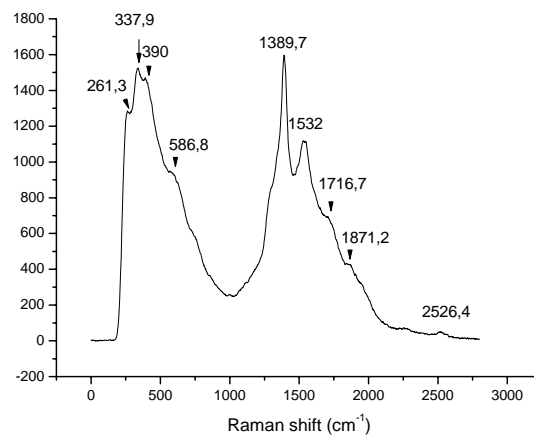


Fig. 8. The Raman spectra for the ZSA type sample, sintered at 1400 °C.

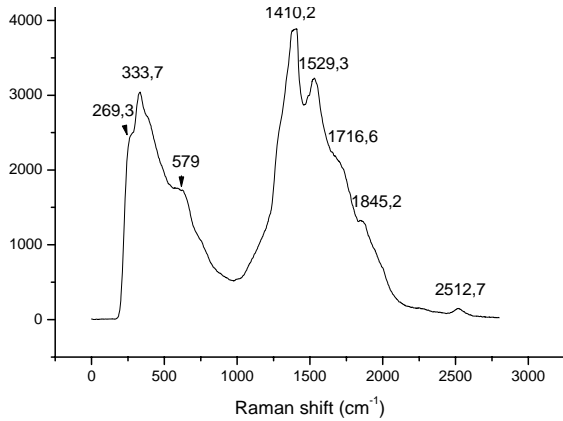


Fig. 9. The Raman spectra for the ZSA type sample, sintered at 1350°C.

The Raman spectra for the S sample is specific for a vitreous structure, which is normally, because this sample have as major compound the silica. The Raman spectra for the MS sample put in evidence the maximum specific to alumina, with the dominant structure associated to the maximum at 1358 cm<sup>-1</sup>, and also the maximum for the mullite and for an amorphous phase of SiO<sub>2</sub>.

The Raman spectra for the MC type samples put in evidence the maximum specific for the alumina, for two types of structure, from whom the dominant is the one associated to the maximum at 1358 cm<sup>-1</sup>, and also the maximum for the magnesium.

For the ZSC samples, the spectra put in evidence the contribution of two phases of ZrO<sub>2</sub> (monoclinic and tetragonal). For the ZSA samples, it appears as dominant the zirconium phases, with a little shift, due to eutectics formation.

The XRD curves are presented in Fig. 10- 13: for the samples MC type – Fig. 10- 11, in the first case being added free Al<sub>2</sub>O<sub>3</sub>, in the second case with no free Al<sub>2</sub>O<sub>3</sub>; for the ZSA type – Fig. 12, and for the ZSC type - Fig. 13.

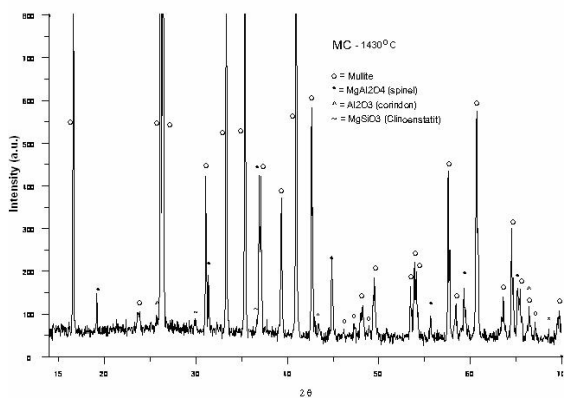


Fig. 10. The XRD curve for the MC composite, treated at 1430°C, with free Al<sub>2</sub>O<sub>3</sub>.

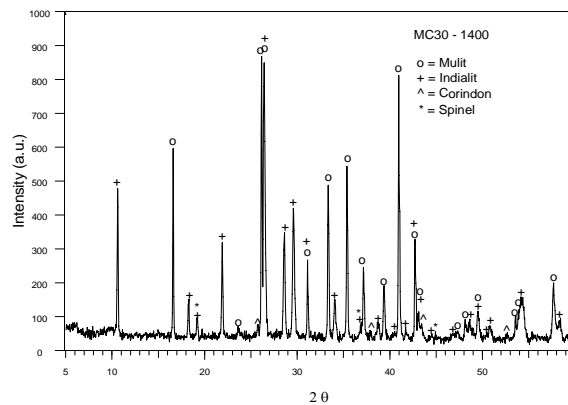


Fig. 11. The XRD curve for MC composite, treated at 1400°C, without free Al<sub>2</sub>O<sub>3</sub>.

In the Fig. 10 there appear the characteristic peaks for mullite- intense and Al<sub>2</sub>O<sub>3</sub>. The MC sample with no free alumina presents intense peaks for cordierite and mullite, smaller quantity- Fig. 11. The treatment temperature is decreased in the second case, and it appears that the cordierite decomposition doesn't take place.

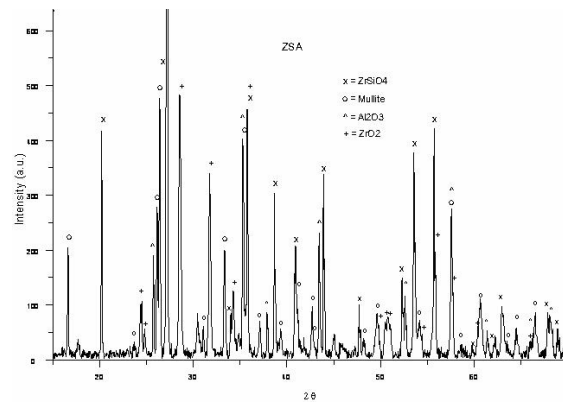


Fig. 12. The XRD spectra for the ZSA composite.

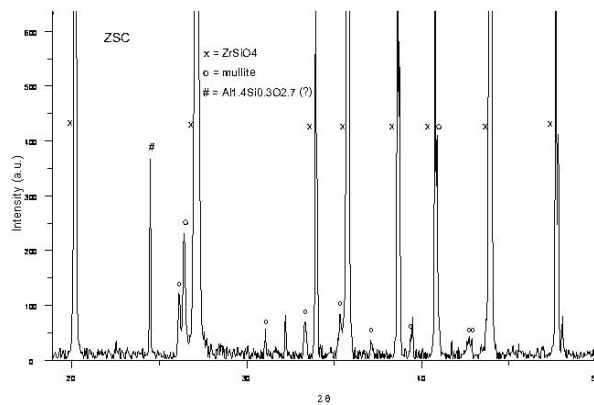


Fig. 13. The XRD spectra for the ZSC composite.

In the case of the ZSA and ZSC composites, it appears the characteristic peaks for zirconium silicate and mullite in both cases. The peaks for Al<sub>2</sub>O<sub>3</sub> and ZrO<sub>2</sub> are present



For the MS sample it can be seen the mullite particles distributed in the vitreous phase. The sintering is advanced. For the MC composite it appear an uniform distribution, without large pores and it can be observed the advanced sintering of the composite particles.

The SEM image for the ZSC and ZSA type samples, thermal treated at 1400 °C are presented, respectively, in Fig. 20 and 21. For the ZSC sample, it can be observed large particles of zirconium silicate, together with long particles of mullite. The structure appears relatively homogeneous, without large pores. For the ZSA composite the particles distribution is more homogeneous than in the case of ZSA, no large pores appears and it can be observed the two type of particles, of zirconium silicate and mullite.

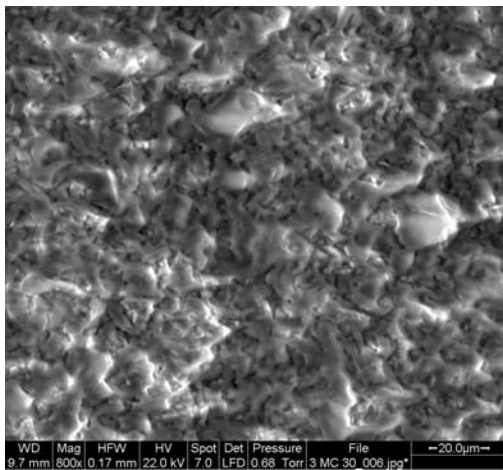


Fig. 19. SEM image for the MC type, sample, burned at 1400 °C.

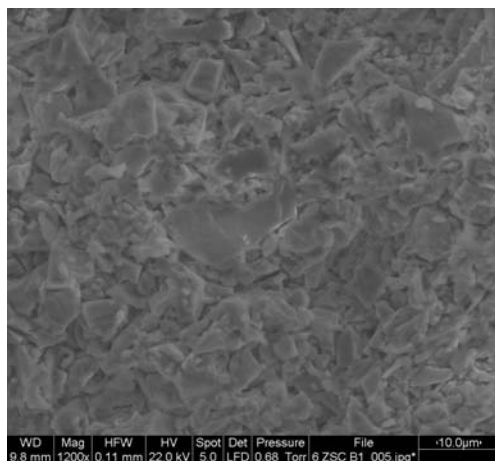


Fig. 20. SEM image of the ZSC type sample, burned at 1400 °C.

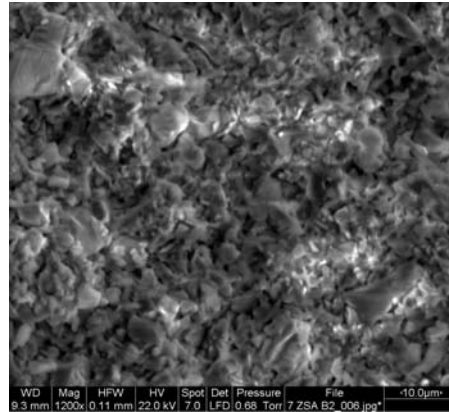


Fig. 21. SEM image of the ZSA type sample, burned at 1400 °C.

#### 4. Conclusions

The best values, respectively the lowest, for the thermal linear expansion index, were those for samples S, MC and MS type, in which both major components have low expansion. The ceramic composite materials MC type are composed mainly from mullite (of 8-10 µm particles dimension) and cordierite (~5 µm). For the MC type sample, the temperature of 1430°C, represents the optimal sintering temperature.

For the ZSC and ZSA type samples, the principal mineralogical compounds are the zirconium oxid, the aluminium oxid and the enstatite. The thermo-mechanical characteristics, characterised by the thermal expansion measurements, in the temperature range from 20 to 920 °C, and the flexural strenght, presents normal values, known from literature from such ceramic materials, for dental technical applications.

For optimal working conditions (sintering temperature of 1430 °C), the medium values for the thermal linear expansion index lies between  $1.9$  and  $5.2 \times 10^{-6} \text{ cm}^{-1}$ , and for the bending resistance the results were within 66 and 93 MPa.

The Raman spectroscopy showed for the S type sample an amorphous structure, and diffuse spectra. For the MC type sample, burned at 1430 °C, they were revealed specific maximum for alumina and mullite, two structures type, from whom that associated to the  $1358 \text{ cm}^{-1}$  maximum is the dominant. For the MS type sample, it was observed a structure similar to that for the MC sample, but in which the  $\text{SiO}_2$  is in amorphous phase. The Raman spectra for ZSC type samples, sintered at 1430, respectively 1400 °C put in evidence the contribution of two phases of  $\text{ZrO}_2$  (monoclinic and tetragonal). The ZSC and ZSA type samples, thermal treated at 1430, 1400 and 1350 °C presents dominant maximum for the zirconium oxide phases, with some displacements and plates, due to eutectics formation.

The increase of the raport cordierite/mullite has benefic influences on the thermo-mechanical properties of the composites. The XRD peaks characteristic to the

cordierite are significant more intense for the increased cordierite amount, and the thermal expansion is lower.

The FTIR spectra reveal the possibility of mixed network, formed by the silicon together with zirconium and aluminium oxides, in the case of ZSC samples. For the MS and MC composites, it appears the characteristic maxima attributed to condensed  $[\text{AlO}_4]$ , at  $800\text{ cm}^{-1}$ . In this case, it is possible that the mixed network is formed by the silicon and aluminium oxides

The scanning electronic microscopy SEM revealed, for the ZSC and ZSA samples, sintered at  $1400\text{ }^\circ\text{C}$ , the mixture of large zirconium silicate particles together with thin mullite ones, in homogeneous and good sintered bodies. For the MS composites, the mullite particles are sintered in vitreous siliceous environment. The MC composites are also good sintered. All the composites show no large pores.

#### Acknowledgement

This paper was supported on the 194(401)/2004 Contract, in the PNCD, MATNANTECH Program, the no 1 Subprogram, MEdC, Romania.

#### References

- [1] H. Schneider, K. Okada, J. A. Pask, *Mullite, Mullite Ceramics*, John Wiley & Sons Chichester, London, (1994).
- [2] K. N. Lee, R. A. Miller, *J. Am. Ceram. Soc.* **79**, 629 (1996).
- [3] P. Fielitz, G. Borchardt, M. Schmocker, H. Schneider, M. Wiedenbeck, D. Rhede, S. Weber, S. Scherrer, *J. Am. Ceram. Soc.* **84**, 2845 (2001).
- [4] P. Fielitz, G. Borchardt, M. Schmocker, H. Schneider, P. Willich, *Applied Surface Science* **203-204**, 639 (2003).
- [5] H. Fritze, J. Jojiu, T. Witke, C. Roscher, S. Weber, S. Scherrer, R. Weiss, B. Schultrich, G. Borchardt, *J. Europ. Ceram. Soc.* **18**, 2351 (1998).
- [6] M. Zhang, E. K. H. Salje, I. Farnan, A. Graeme-Barber, P. Daniel, R. C. Ewing, A. M. Clark, H. Leroux, *J. Phys. Condens. Matter*, **12**, 1915 (2000).
- [7] M. Zhang, E. K. H. Salje, G. C. Capitani, H. Leroux, A. M. Clark, J. Schluter, R. C. Ewing, *J. Phys. Condens. Matter*, **12**, 3131 (2000).
- [8] EnHai Sun, Yong-Ho Choa, Tohru Sekino, Koichi Niihara, *Journal of Ceramic Processing Research* **1**, 9 (2000).

\*Corresponding author: savabogdanalexandru@yahoo.com